Supporting Information

Elongated Lifetime and Enhanced Flux of Hot Electrons on Perovskite Plasmonic Nanodiode

Yujin Park[1,2], Jungkweon Choi[1,2,3], Changhwan Lee[2,4], An-Na Cho[5], Dae Won Cho[6], Nam-Gyu Park[5], Hyotcherl Ihee[1,2,3*] and Jeong Young Park[1,2,4*]

[1]*Department of Chemistry, Korea Advanced Institute of Science and Technology (KAIST), Daejeon 305-701, Republic of Korea*

[2]*Center for Nanomaterials and Chemical Reactions, Institute for Basic Science (IBS), Daejeon 305-701, Republic of Korea*

[3]*KI for the BioCentury, Korea Advanced Institute of Science and Technology (KAIST), Daejeon 305-701, Republic of Korea*

[4]*Graduate School of EEWS, Korea Advanced Institute of Science and Technology (KAIST), Daejeon 305-701, Republic of Korea*

[5]*School of Chemical Engineering and Department of Energy Science, Sungkyunkwan University, Suwon 440-746, Republic of Korea*

[6]*Department of Advanced Materials Chemistry, Korea University, Sejong Campus, Sejong 30019, Republic of Korea*

*To whom correspondence should be addressed. E-mail: hyotcherl.ihee@kaist.ac.kr, jeongypark@kaist.ac.kr

Keywords: Hot electron, inorganic-organic hybrid perovskite, surface plasmon, Schottky nanodiode, hot carrier solar cells

Methods

1. Fabrication and Characterization of the $MAPbI_3$-Modified Au/TiO_2 Nanodiode.

To obtain a steady-state hot electron current, it is necessary to make a nanodiode. The procedure to fabricate the $MAPbI_3$-modified Au/TiO_2 nanodiode can be divided into three processes: (i) synthesize the perovskite precursor ink, (ii) prepare the Au/TiO_2 nanodiode, and (iii) finally, spin coat the perovskite precursor ink on top of the Au/TiO_2 nanodiode.

Synthesis of the $MAPbI_3$ Precursor Ink A more detailed description of the chemical and synthesis processes used in this work can be found in Ahn et al.[1] First, 26.86 ml of methylamine (40 wt% in methanol, TCI) and 30 ml of hydriodic acid (57 wt% in water, Sigma-Aldrich) were reacted at 0 ℃ for 2 h to obtain methylammonium iodide (CH_3NH_3I) powder. The white CH_3NH_3I powder was then recovered at 60 ℃ using a rotary evaporator. This powder was washed with ether (99%, Samchun) and stored in a vacuum oven at 60 ℃ overnight. Next, the CH_3NH_3I powder (318 mg), PbI_2 (922mg, 99.99%, TCI), and N,N-dimethylsulfoxide (142 μl, 99.5%, Sigma-Aldrich) were dissolved in N,N-diemthylformamide (1048 μl, 99.8%, Sigma-Aldrich) to make the $MAPbI_3$ precursor ink. The $MAPbI_3$ precursor ink was stirred thoroughly in air until fully dissolved.

Fabrication of the Thin-Film-Au/TiO_2 and Plasmonic-Au/TiO_2 Nanodiode We made two types of Au: thin-film and plasmonic. To fabricate the thin-film-Au/TiO_2 nanodiode, a patterned stainless-steel mask (4×7 mm^2) was aligned on an insulating silicon oxide wafer (300 nm), and then a Ti film (150 nm) was deposited using e-beam evaporation. The deposited Ti layer was heated at 470 ℃ in air for 2 h 15 min to react to form the TiO_2 layer. After that, two ohmic electrodes composed of Ti (50 nm) and Au (100 nm) were evaporated with a second patterned mask (5×5 mm^2), for the ohmic junction with the titanium oxide layer and the top gold film, respectively. Finally, the top thin layer of Au (15 nm) was deposited with a third patterned mask (2×6 mm^2). For the plasmonic-Au/TiO_2 nanodiode, the thin-film-Au/TiO_2 nanodiode was annealed at 200 °C for an hour in ambient air.

Fabrication of the $MAPbI_3$-Modified Au/TiO_2 Nanodiode To fabricate the $MAPbI_3$-modified Au/TiO_2 nanodiode, the prepared perovskite precursor ink was diluted to make a thin

$MAPbI_3$ layer. After that, the diluted precursor ink (20 μl) was spin-coated on the surface of the active area at 4000 rpm for 25 sec. During the spin-coating process, 0.7 ml of diethyl ether (99.7%, anhydrous, Sigma-Aldrich) was gradually dropped onto the sample surface for 10 sec. The spin-coated perovskite film was then heated at 60 ℃ for 1 min and at 100 ℃ for 9 min in air. Finally, the nanodiode was cleaned with a solvent (except the top Au layer) to remove any unnecessary perovskite layer. The active area of the fabricated nanodiode is 2 × 2 mm^2, and the samples were kept under N_2 to avoid degradation of the perovskite film.

Sample Preparation for the Femtosecond Transient Absorption (TA) Experiments Samples must absorb sufficient incident photons to obtain proper TA results, so we modified the sample fabrication process to generate thicker layers. Transparent quartz (2 × 2 cm^2) was used as the substrate, and the TiO_2 layer was made by heating a Ti film (80 nm) at the same temperature and time as in the nanodiode fabrication method. A gold film (20 nm) was deposited for the thin-film Au samples, and plasmonic Au was made by heating a 12.5 nm Au layer at 200 ℃ for 1 h in air. For a thicker perovskite layer, a 300 mM solution of precursor ink was prepared and spin-coated 5 times at the same conditions as used in the nanodiode fabrication process.

Characterization The current–voltage curves and short-circuit photocurrents were measured using a source meter (Keithley instrument 2400). A tungsten–halogen lamp with a broad visible light spectrum and intensity of 9 mW/cm^2 was used as the incident light source. The incident photon-to-current conversion efficiency (IPCE) was characterized with a Xe arc lamp source, where the wavelength can be tuned from 380 to 900 nm (Newport, TLS-300XU). The absorbance spectrum of the fabricated nanostructures was obtained using an UV-vis spectrophotometer (Hitachi, UV3600), and a clean quartz window was used as the reference. The sub-picosecond time-resolved absorption spectra were collected using a pump-probe transient absorption spectroscopy system. The pump light was generated by using a regenerative amplified titanium sapphire laser system (Spectra Physics, Spitfire Ace, 1 kHz) pumped by a diode-pumped Q-switched laser (Spectra Physics, Empower). The seed pulse was generated using a titanium sapphire laser (Spectra Physics, MaiTai SP). For the excitation beam, 420 nm pulses produced from an optical parametric amplifier (Spectra Physics, TOPAS prime)

were used. The residual of the fundamental beam was converted to a white light continuum pulse, which was employed as the probe pulse with a controlled optical delay. The transmitted probe pulse was detected for spectral measurement with a CCD detector attached to an absorption spectroscope. The mechanical chopper modulated the pump pulse to obtain a pair of spectra with and without excitation, so the difference in absorption could be estimated.

2. Structures of the Fabricated $MAPbI_3$/Thin-Film-Au/TiO_2 and $MAPbI_3$/Plasmonic-Au/TiO_2 Nanodiodes.

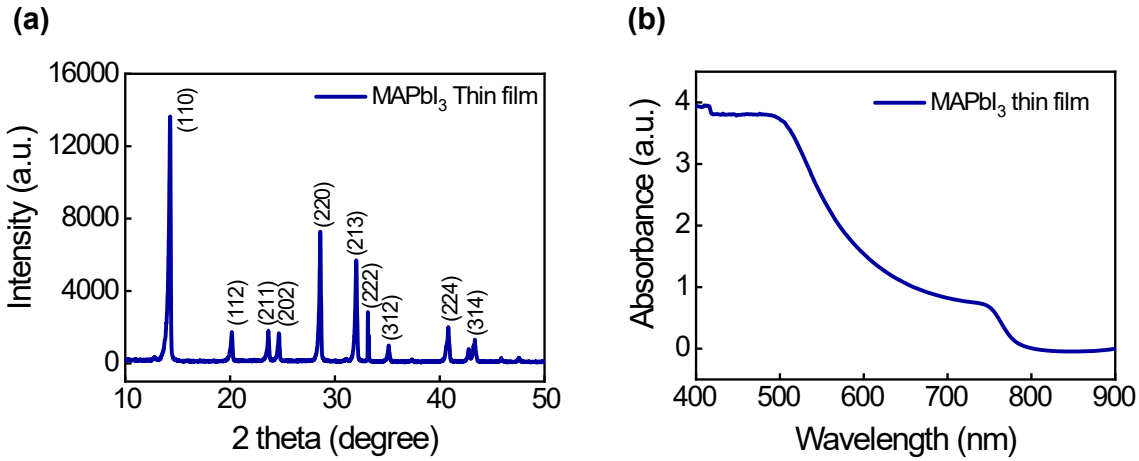

Figure S1. (a) XRD patterns and (b) absorbance spectrum of the $MAPbI_3$ thin film.

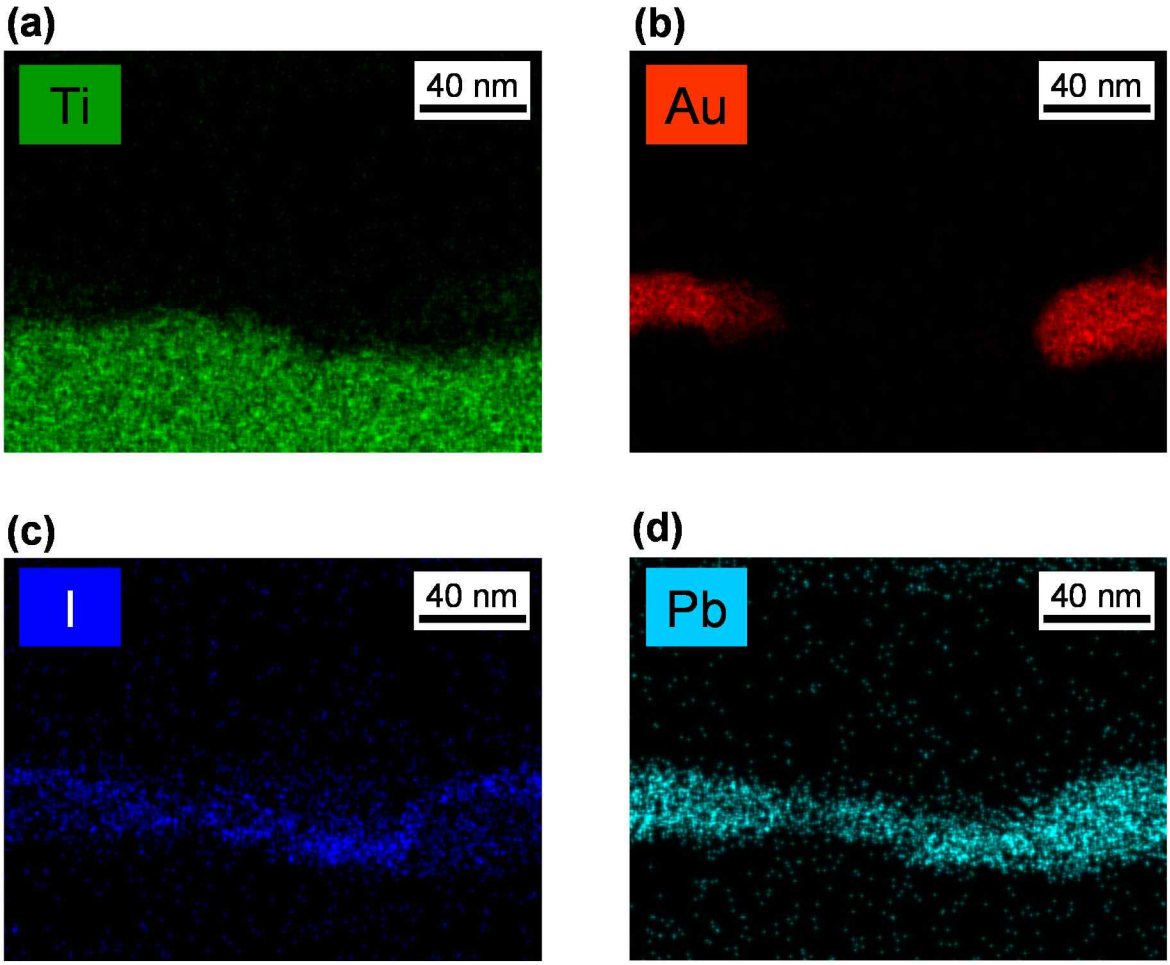

Figure S2. EDS elemental mapping images of the $MAPbI_3$/plasmonic-Au/TiO_2 nanodiode. The images correspond to (a) Ti, (b) Au, (c) I, and (d) Pb.

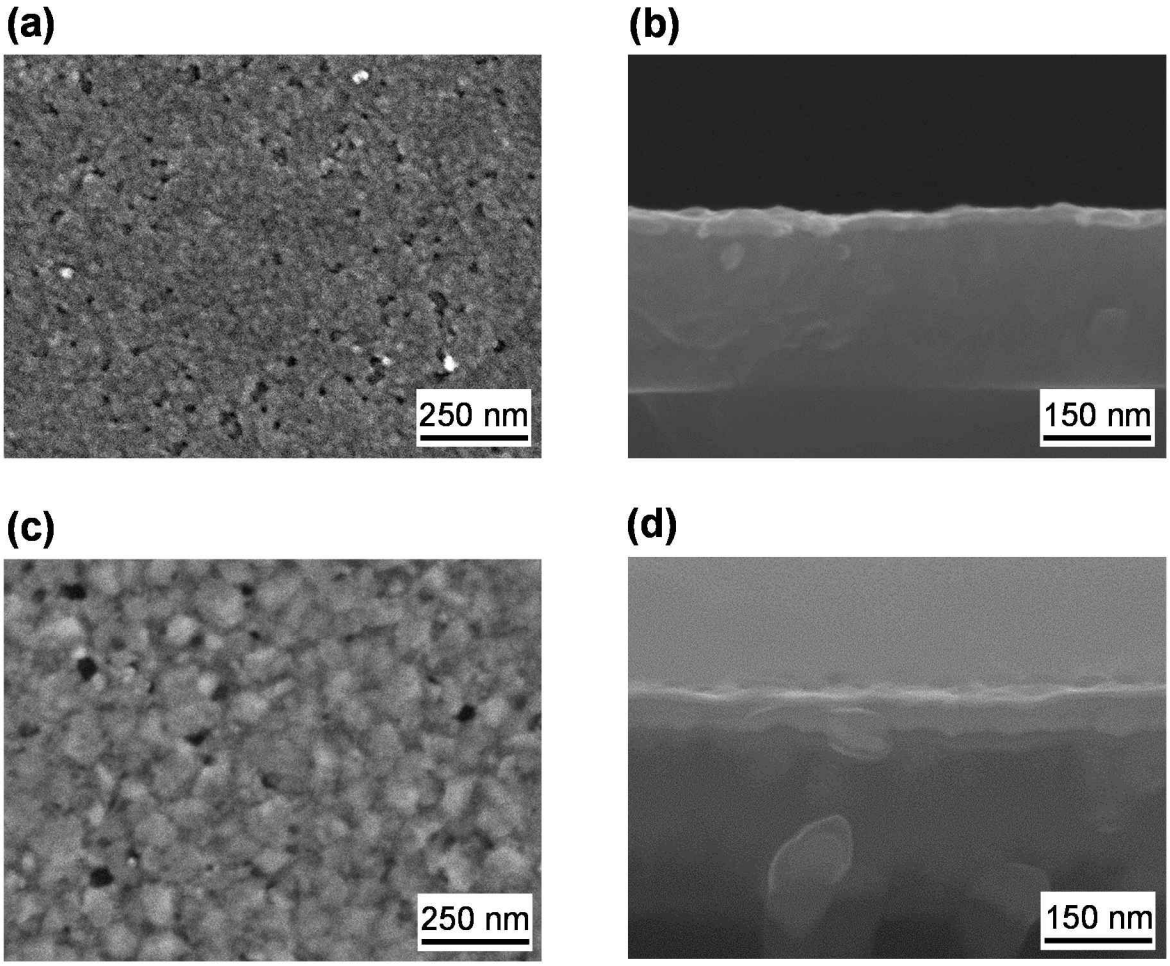

Figure S3. (a) Plane view and (b) cross-sectional view of the scanning electron microscopy (SEM) images of the bare thin-film-Au/TiO_2 nanodiode. SEM images of the $MAPbI_3$/thin-film-Au/TiO_2 nanodiode in (c) plane view and (d) cross-sectional view.

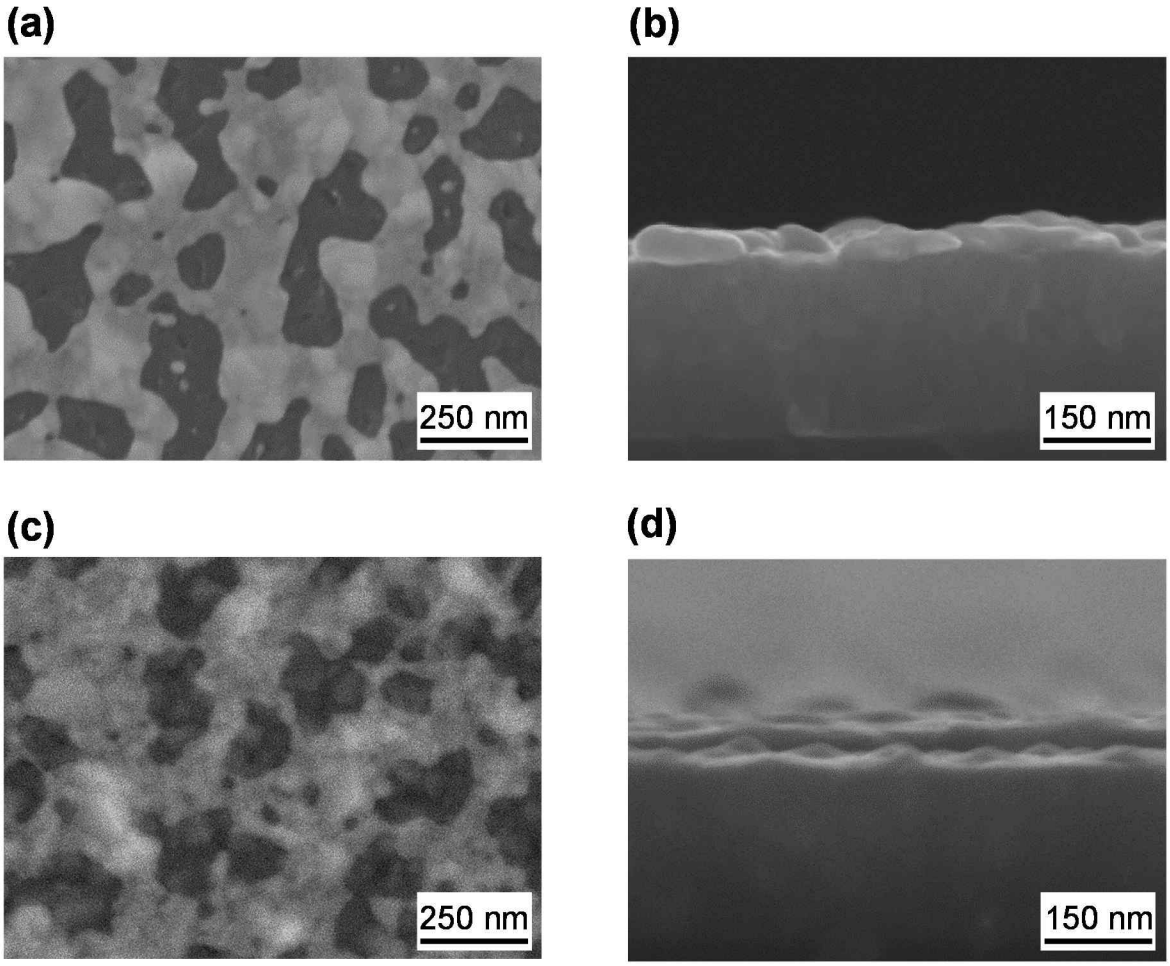

Figure S4. (a) Plane view and (b) cross-sectional view of the SEM images of the bare plasmonic-Au/TiO_2 nanodiode. SEM images of the $MAPbI_3$/plasmonic-Au/TiO_2 nanodiode in (c) plane view and (d) cross-sectional view.

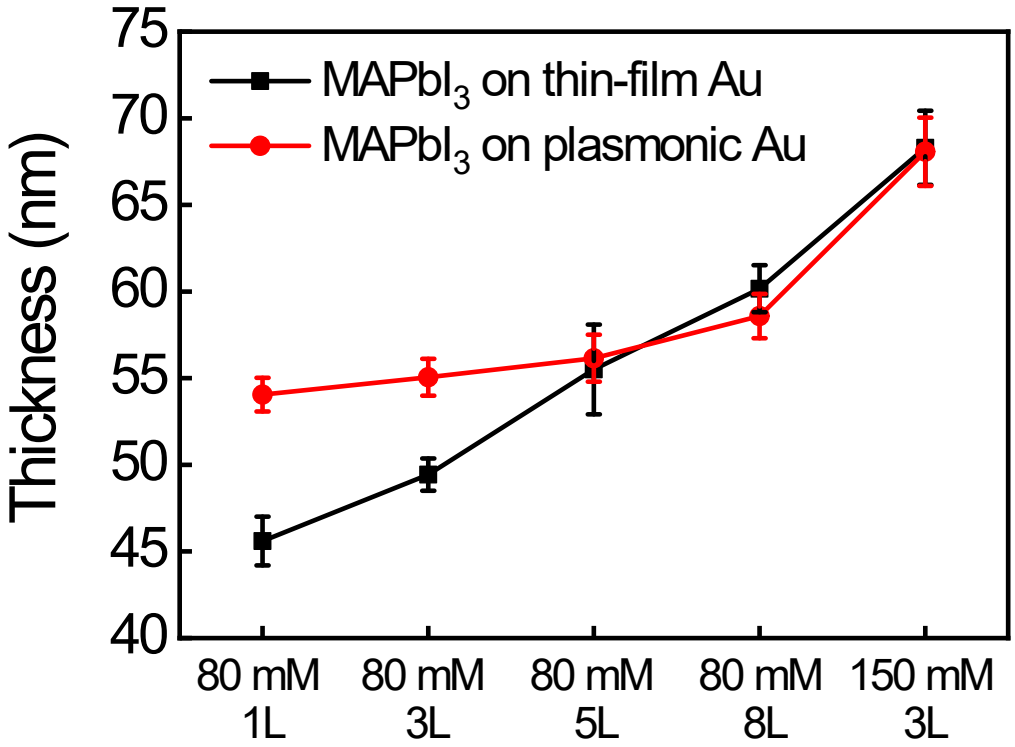

Figure S5. Thickness of the $MAPbI_3$ layer according to the number of repeated $MAPbI_3$ deposition steps on the thin-film Au and plasmonic Au.

3. I–V Curves and Calculated Schottky Barrier Heights of the Fabricated Nanodiodes.

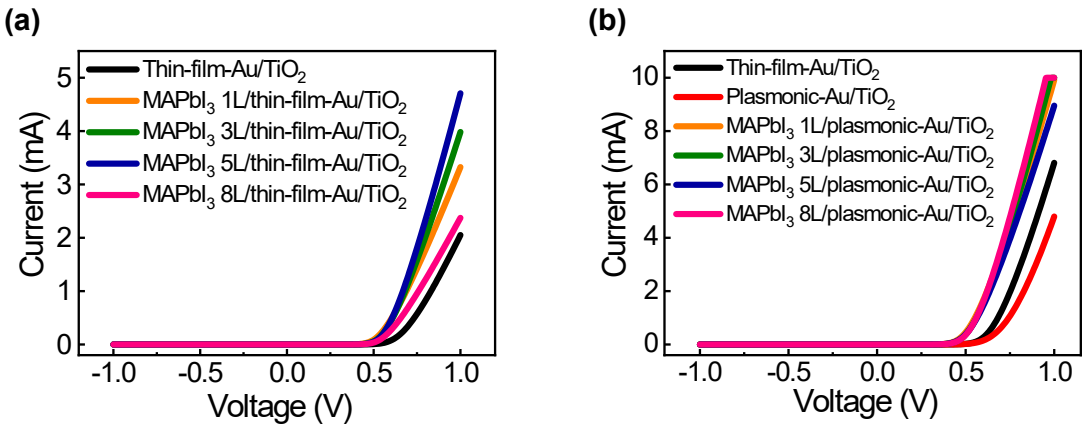

Figure S6. Current–voltage (I–V) curves measured on the (a) $MAPbI_3$/thin-film-Au/TiO_2 and (b) $MAPbI_3$/plasmonic-Au/TiO_2 nanodiodes showing their respective rectifying behavior.

We can obtain Schottky barrier heights, ideality factors, and series resistance for the fabricated nanodiodes by fitting measured I–V curves with the thermionic emission equation. The current density induced by overcoming the Schottky barrier height by thermionic emission as a function of external voltage is given by

$$I = AA^{**}T^2 exp\left(-\frac{qE_{SB}}{k_bT}\right)\left[exp\left(\frac{q(V-IR_s)}{\eta k_bT}-1\right)\right]$$

where A is the area, A^{**} is the effective Richardson constant, E_{SB} is the Schottky barrier height, k_b is the Boltzmann constant, T is the temperature, R_s is the series resistance, and η is the ideality factor.

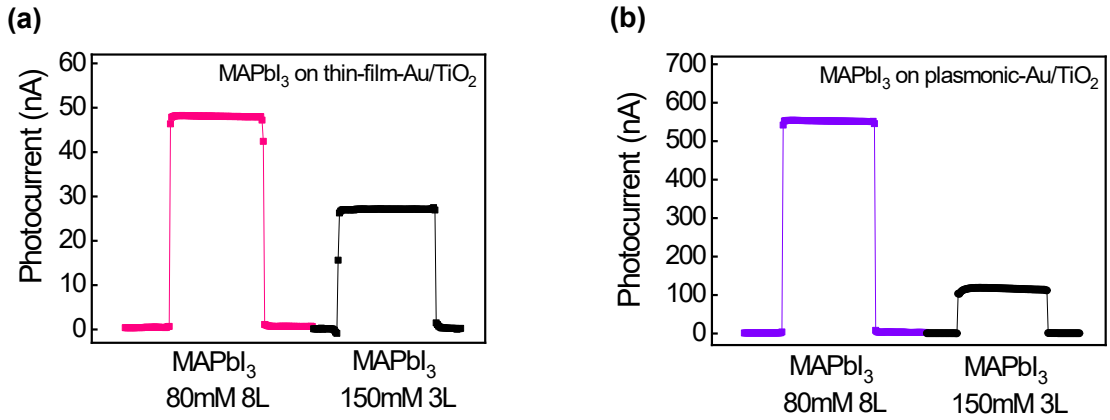

Figure S7. The short-circuit photocurrent detected on the (a) $MAPbI_3$/thin-film-Au/TiO_2 and (b) $MAPbI_3$/plasmonic-Au/TiO_2 nanodiodes with different thicknesses of $MAPbI_3$. The photocurrent diminishes with a thicker perovskite layer (~70 nm) because of the mean free path length of the hot electrons.

4. Demonstration of the LSPR Effect on Photo-Conversion Performance.

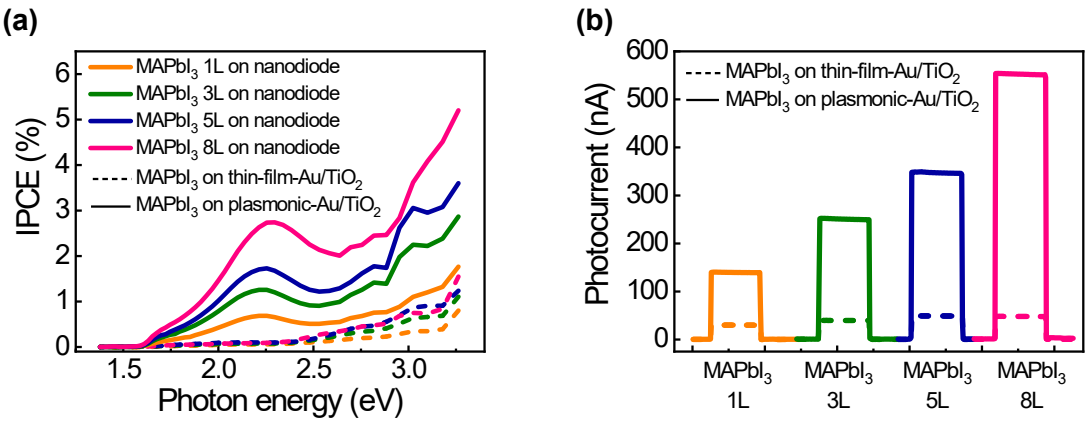

Figure S8. Plots comparing the (a) IPCE and (b) short-circuit photocurrent detected on the $MAPbI_3$/thin-film-Au/TiO_2 and $MAPbI_3$/plasmonic-Au/TiO_2 photo-nanodiodes with identical perovskite deposition.

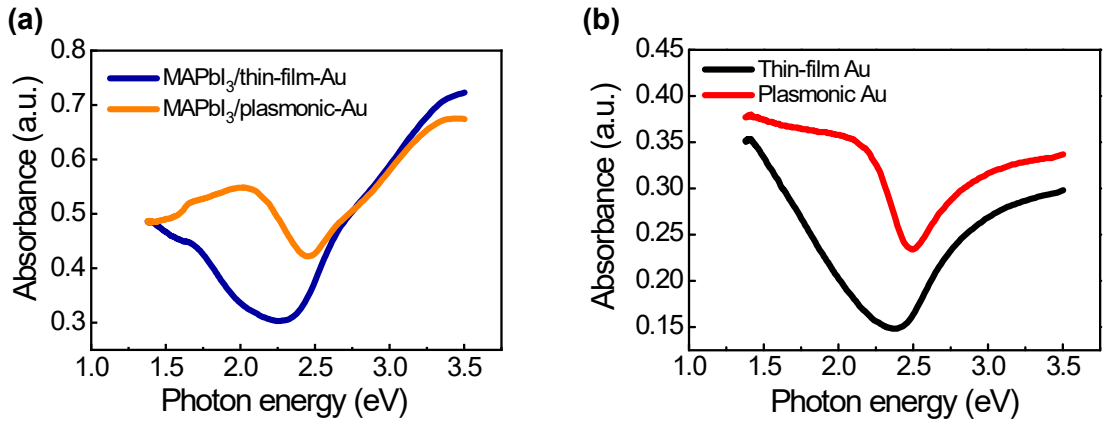

Figure S9. Absorbance spectra of (a) the $MAPbI_3$/thin-film-Au and $MAPbI_3$/plasmonic-Au, and of (b) the bare thin-film Au and plasmonic Au.

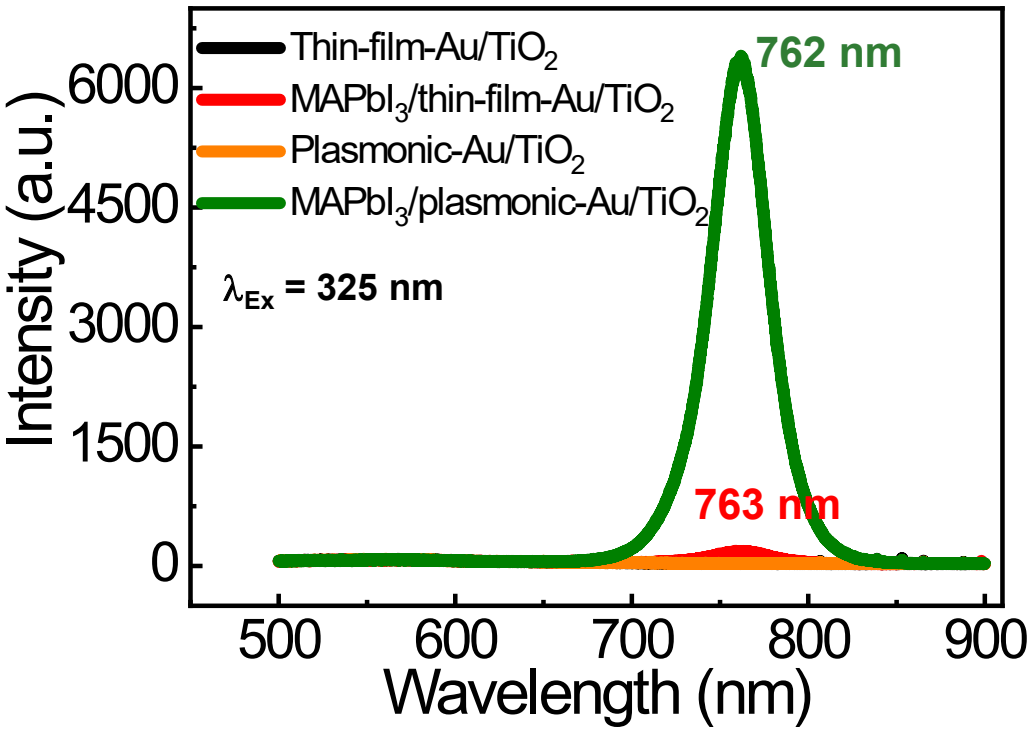

Figure S10. Photoluminescence (PL) spectra of the thin-film-Au/TiO_2 (black), $MAPbI_3$/thin-film-Au/TiO_2 (red), plasmonic-Au/TiO_2 (orange), and $MAPbI_3$/plasmonic-Au/TiO_2 (green) with an excitation wavelength at 325 nm.

5. Characterization of the Samples Used for the Femtosecond Transient Absorption (TA) Experiments.

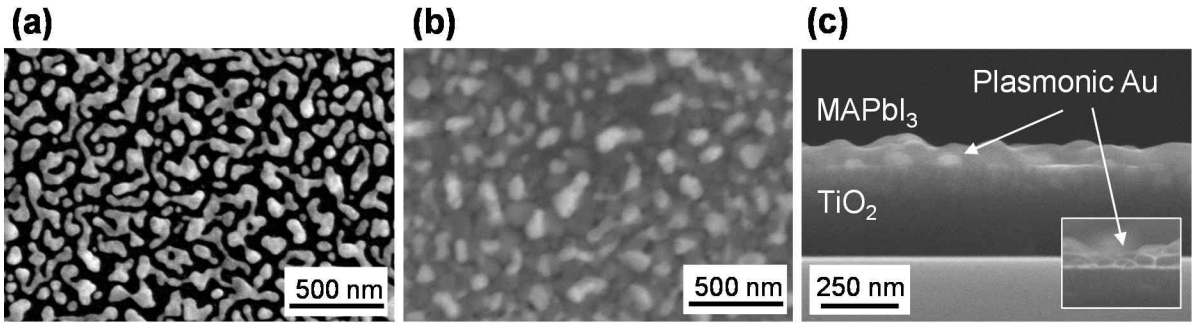

Figure S11. SEM images of the structures used for the TA experiments. (a) Bare plasmonic-Au/TiO_2 on quartz. $MAPbI_3$/plasmonic-Au/TiO_2 deposited on quartz (b) in plane view and (c) cross-sectional view. Inset image in (c) shows the bare plasmonic-Au/TiO_2 structure in cross-sectional view.

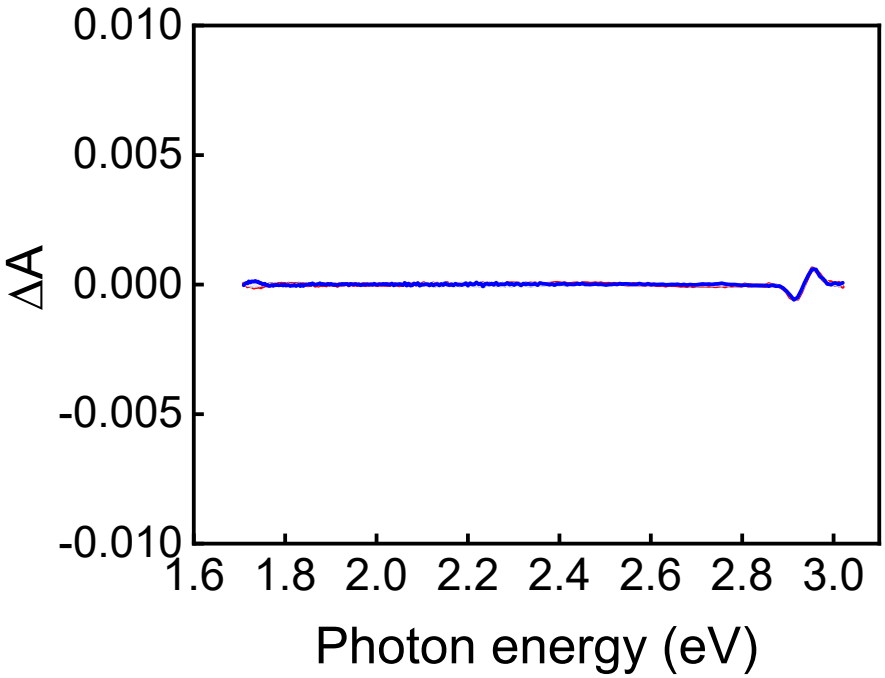

Figure S12. TA spectra of TiO_2 deposited on quartz with photoexcitation at 3.0 eV.

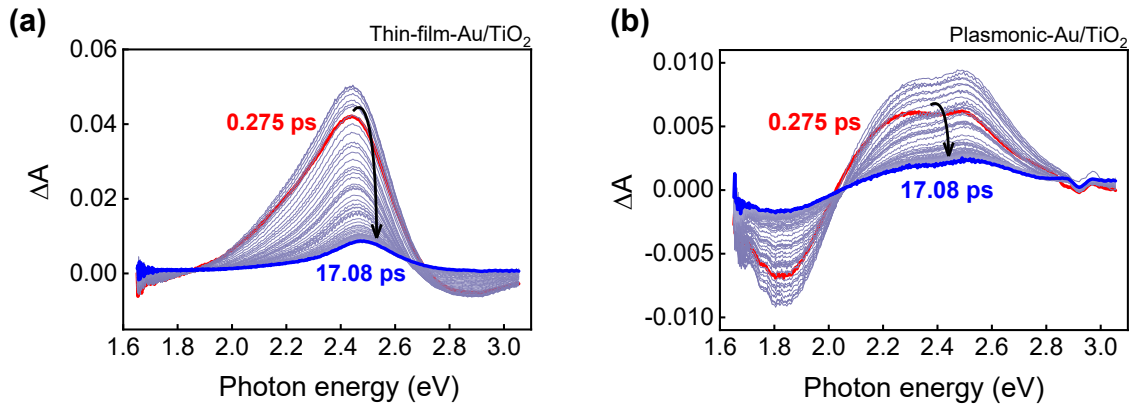

Figure S13. TA spectra of (a) thin-film-Au/TiO_2 and (b) plasmonic-Au/TiO_2 structures with photoexcitation at 3.0 eV.

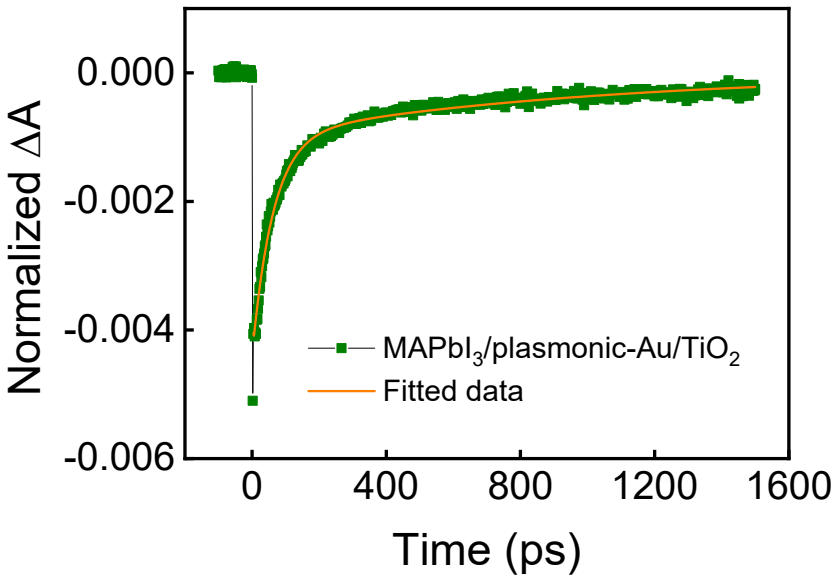

Figure S14. Decay profile of the $MAPbI_3$/plasmonic-Au/TiO_2 structure probed with longer delay times.

Table S1. Parameters calculated from fitting the I–V curves measured on (a) the $MAPbI_3$/thin-film-Au/TiO_2 and (b) $MAPbI_3$/plasmonic-Au/TiO_2 nanodiodes to the thermionic emission equation.

(a)

	Schottky barrier height (E_{SB})	**Ideality factor (η)**	**Series resistance (R_s)**
Thin-film-Au	0.87 eV	1.67	131.2 Ω
$MAPbI_3$ 1L/ thin-film-Au	0.861 eV	1.41	115.4 Ω
$MAPbI_3$ 1L/ thin-film-Au	0.871 eV	1.41	89.8 Ω
$MAPbI_3$ 1L/ thin-film-Au	0.871 eV	1.42	73.9 Ω
$MAPbI_3$ 1L/ thin-film-Au	0.879 eV	1.42	152 Ω

(b)

	Schottky barrier height (E_{SB})	**Ideality factor (η)**	**Series resistance (R_s)**
Thin-film-Au	0.858 eV	1.59	40.8 Ω
Plasmonic-Au	0.764 eV	2.27	43.2 Ω
$MAPbI_3$ 1L/ plasmonic-Au	0.770 eV	1.64	39.15 Ω
$MAPbI_3$ 3L/ plasmonic-Au	0.777 eV	1.63	36 Ω
$MAPbI_3$ 5L/ plasmonic-Au	0.78 eV	1.61	43.1 Ω
$MAPbI_3$ 8L/ plasmonic-Au	0.792 eV	1.56	33.2 Ω